On the Meaning of Affinity: Cluster Glycoside Effects and Concanavalin A

Sarah M. Dimick,[†] Steven C. Powell,[†] Stephen A. McMahon,[‡] Davina N. Moothoo,[‡] James H. Naismith,*[,‡] and Eric J. Toone*[,†]

Contribution from the Department of Chemistry, Duke University, Durham, North Carolina 27708-0346, and Center for Biomolecular Science, Purdie Building, The University, St. Andrews KY16 9ST, Scotland, U.K.

Received May 24, 1999

Abstract: The inhibition of protein−carbohydrate interaction provides a powerful therapeutic strategy for the treatment of myriad human diseases. To date, application of such approaches have been frustrated by the inherent low affinity of carbohydrate ligands for their protein receptors. Because lectins typically exist in multimeric assemblies, a variety of polyvalent saccharide ligands have been prepared in the search for high affinity. The cluster glycoside effect, or the observation of high affinity derived from multivalency in oligosaccharide ligands, apparently represents the best strategy for overcoming the "weak binding" problem. Here we report the synthesis of a series of multivalent dendritic saccharides and a biophysical evaluation of their interaction with the plant lectin concanavalin A. Although a 30-fold enhancement in affinity on a valence-corrected basis is observed by agglutination assay, calorimetric titration of soluble protein with a range of multivalent ligands reveals no enhancement in binding free energies. Rather, IC_{50} values from agglutination measurements correlate well with *entropies* of binding. This observation suggests that hemagglutination measures a phenomenon distinct from binding that is typified by a large favorable entropy and an unfavorable enthalpy: this process is almost certainly aggregation. Supporting this assertion, we report crystal structures of multivalent ligands cross-linking concanavalin A dimers. To the best of our knowledge, these structures are the first reported of their kind. Our results indicate that hemagglutination assays evaluate the ability of ligands to inhibit the formation of cross-linked lattices, a process only tangentially related to reversible ligand binding. Cluster glycoside effects observed in agglutination assays must, therefore, be viewed with caution. Such effects may or may not be relevant to the design of therapeutically useful saccharides.

Introduction

The initiation of a wide range of human diseases is mediated by protein−carbohydrate recognition.[1−7] In the earliest phases of infection by a variety of viral, parasitic, mycoplasmal, and bacterial pathogens, host recognition is achieved through specific adhesion to cell surface carbohydrate epitopes. Protein−carbohydrate interaction also plays a major role in the progression of many human cancers, contributing to both random and nonrandom metastatic events.[8,9] Because of the myriad and varied roles of protein−carbohydrate interaction in human disease, the development of small-molecule inhibitors of pathogenic saccharide-mediated adhesion has been the subject of intense activity in recent years. The paradigm is an attractive one since it would provide a non-cytotoxic group of therapeutic products applicable to a wide range of human diseases.

Despite the intellectual appeal of the methodology, construction of such compounds is hampered by several fundamental concerns. Chief among these is the low-affinity binding that typifies protein−carbohydrate interaction: such binding events proceed uniformly with millimolar to micromolar dissociation constants.[10] Accordingly, a major focus of contemporary carbohydrate research surrounds the development of general strategies for increasing lectin−ligand binding affinities to the levels required for therapeutic use.

Lectins are seldom found in vivo as monomeric species; rather, they typically exist as oligomeric structures. This phenomenon suggests that Nature has dealt with the "tight binding" problem through multivalency, where multiple simultaneous binding events overcome weak individual interaction free energies. A straightforward corollary of this hypothesis is that synthetic polyvalent ligands should show high binding affinities. From this basis, several groups have pursued the goal of tight lectin−ligand binding through multivalency, and a number of ligands with valencies from 2 to 20 have been prepared for binding to a variety of lectins.[11−16] Lee and coworkers have prepared a series of multivalent mannosides as

[†] Duke University.
[‡] The University, St. Andrews.

(1) Hughes, R. C. *Curr. Opin. Struct. Biol.* **1992**, *2*, 687.
(2) Drickamer, K.; Taylor, M. E. *Annu. Rev. Cell Biol.* **1993**, *9*, 237.
(3) Lee, Y. C.; Lee, R. T. *J. Biomed. Sci.* **1996**, *3*, 221.
(4) Dwek, R. A. *Chem. Rev.* **1996**, *96*, 683.
(5) Wong, S. Y. C. *Curr. Opin. Struct. Biol.* **1995**, *5*, 599.
(6) Cook, G. M. W. *Glycobiology* **1995**, *5*, 449.
(7) Kobata, A. *Acc. Chem. Res.* **1993**, *26*, 319.
(8) Beuth, J.; K., H. L.; Pulverer, G.; Uhlenbruck, G.; Pichlmaier, H. *Glycoconjugate J.* **1995**, *12*, 1.
(9) Gabius, H.-J.; Kayser, K.; Gabius, S. *Naturwissenschaften* **1995**, 82, 533.
(10) Toone, E. J. *Curr. Opin. Struct. Biol.* **1994**, *4*, 719.
(11) Roy, R. *Polym. News* **1996**, *21*, 226.
(12) Roy, R. *Curr. Opin. Struct. Biol.* **1996**, *6*, 692.
(13) Roy, R. *Topics Curr. Chem.* **1997**, *187*, 241.
(14) Rini, J. M. *Annu. Rev. Biophys. Biomol. Struct.* **1995**, *24*, 551.
(15) Kiessling, L. L.; Pohl, N. L. *Chem. Biol.* **1996**, *3*, 71.
(16) Drickamer, K. *Struct. Biol.* **1995**, *2*, 437.

10.1021/ja991729e CCC: $18.00
Published on Web 10/14/1999

ligands for the mannose binding protein: the tightest-binding of this group show enhancements of 10^3-10^4 over the monovalent ligand.[17,18] Biessen and co-workers prepared a hexavalent mannoside for the same protein that showed a valence-corrected enhancement in binding affinity of 10^5 over methyl α-D-mannopyranoside.[19] Roy and co-workers have prepared a variety of polyvalent saccharides for various plant lectins and for the influenza hemagglutinin.[20−25] In general, these ligands show enhancements of $10-10^3$ over the appropriate monovalent ligand. Another class of polyvalent glycosidic ligands, the so-called glycopolymers, provide even more spectacular enhancements in affinity. A series of acrylamide/acrylic acid ester copolymers show enhancements in affinity to 10^9, again on a valence-corrected or per mole of saccharide basis.[26−31] The sometimes spectacular successes of this strategy have led to general acceptance of the "cluster glycoside" effect, defined as "an affinity enhancement over and beyond what would be expected from the concentration increase of the determinant sugar in a multivalent ligand".[17,32]

Despite the phenomenological success of multivalency strategies, a molecular interpretation of the effect is difficult. Typically, cluster glycoside effects are interpreted in terms of entropic advantage, either an effective concentration argument or a chelate effect. However, in many examples the linker region between recognition epitopes is too short to span two binding sites. Cluster glycoside effects have been observed for monovalent lectins, although the lectins were immobillized on microtiter plate wells.[33−35] On its face, an entropic enhancement to valence-corrected binding free energies seems unlikely. The binding free energy for a bivalent ligand to a bivalent receptor is related to the analogous monovalent binding free energies by the expression

$$\Delta G = 2\Delta G_m + \Delta G_i$$

where ΔG_m represents the binding free energy of the component monovalent ligands and ΔG_i is an interaction energy, the energetic consequence of physical linkage of the monovalent recognition domains.[36] Assuming the linker domain is of sufficient length and flexibility to allow optimal localization of the receptor domains in their appropriate binding sites, enthalpic contributions to ΔG_i will be small. Rather, the dominant contributions to interaction energies arise from entropic effects. Specifically, two terms with opposite signs contribute to ΔG_i. First, tethering of recognition domains reduces the overall translational and rotational entropy of binding. During complete binding of a bivalent receptor by monovalent ligand, three particles are converted to one; during the corresponding binding of a bivalent ligand, two particles are converted to one. Binding of a bivalent ligand thus proceeds with an entropic "savings" equivalent to the translational and rotational entropy of one monovalent ligand. The magnitude of this effect is difficult to accurately ascertain: current estimates of the translational and rotational entropy barrier to bimolecular complex formation in aqueous solution range from 2.5 to 15 kcal mol^{-1} near room temperature.[37−40] Countering this effect, the introduction of a flexible linker region introduces an entropic penalty relative to monovalent ligand binding as conformational degrees of freedom in the linker domain are frozen out during binding. Again, the exact magnitude of this effect is difficult to estimate, although the smallest estimates lie in the vicinity of 0.5 kcal mol^{-1} per rigid rotor frozen during binding.[41−44] Given that distances between carbohydrate binding sites on most polyvalent lectins range from 20 to 70 Å, it seems unlikely that a chelate effect could provide an enhancement to reversible binding free energies. At this time, then, the molecular basis for the cluster glycoside effect is not well understood.

Efforts to provide a molecular basis for the cluster glycoside effect have been frustrated by two issues: (i) polyvalent ligands are often polydisperse and structurally ill-defined and (ii) assays typically used to evaluate protein−carbohydrate binding—especially those based on aggregation of macromolecules—measure several molecular phenomena including, but not limited to, reversible thermodynamic protein−carbohydrate association. Here we describe experiments designed to provide a molecular basis for the cluster glycoside effect. Below we detail the preparation and characterization of a series of dendritic ligands for the plant lectin concanavalin A. We have characterized the interaction of polyvalent ligands with this lectin through agglutination assays, titration microcalorimetry, low-angle dynamic light scattering, and X-ray crystallography. Together the results of these studies allow a concise and unambiguous interpretation of multivalency effects in protein−carbohydrate interaction.

Results and Discussion

Synthesis of Ligands. We have chosen the plant lectin concanavalin A as a model lectin for our studies. Lectins are ubiquitous in plants, and a wide range of mannose-specific lectins have been isolated from the seeds of legumes. The best known of these proteins is concanavalin A (con A), first isolated and crystallized some 60 years ago from the seeds of *Canavalia*

(17) Lee, Y. C.; Lee, R. T. *Acc. Chem. Res.* **1995**, *28*, 321.
(18) Quesenberry, M. S.; Lee, R. T.; Lee, Y. C. *Biochemistry* **1997**, *36*, 2724.
(19) Biessen, E. A. L.; Noorman, F.; van Teijlingen, M. E.; Kuipert, J.; Barrett-Bergshoeff, M.; Bijsterbosch, M. K.; Rijken, D. C.; van Berkel, T. J. C. *J. Biol. Chem.* **1996**, *271*, 28030.
(20) Pagé, D.; Zanini, D.; Roy, R. *Bioorg. Med. Chem.* **1996**, *4*, 1949.
(21) Meunier, S. J.; Roy, R. *Tetrahedron Lett.* **1996**, *37*, 5469.
(22) Page, D.; Aravind, S.; Roy, R. *J. Chem. Soc., Chem. Commun.* **1996**, 1913.
(23) Zanini, D.; Roy, R. *Bioconjugate Chem.* **1997**, *8*, 187.
(24) Zanini, D.; Roy, R. *J. Org. Chem.* **1996**, *61*, 7348.
(25) Zanini, D.; Park, W. K. C.; Roy, R. *Tetrahedron Lett.* **1995**, *36*, 7383.
(26) Sigal, G. B.; Mammen, M.; Dahmann, G.; Whitesides, G. M. *J. Am. Chem. Soc.* **1996**, *118*, 3789.
(27) Mammen, M.; Dahmann, G.; Whitesides, G. M. *J. Med. Chem.* **1995**, *38*, 4179.
(28) Matrosovich, M. N.; Mochalova, L. V.; Marinina, V. P.; Byramova, N. E.; Bovin, N. V. *FEBS Lett.* **1990**, *272*, 209.
(29) Roy, R.; Laferriere, C. A. *Carbohydr. Res.* **1988**, *177*, C1.
(30) Gamian, A.; Chomik, M.; Laferriere, G. A.; Roy, R. *Can. J. Micorbiol.* **1991**, *37*, 233.
(31) Watson, J. L.; Spaltenstein, A.; Kingery-Wood, J. E.; Whitesides, G. M. *J. Med. Chem.* **1994**, *37*, 3419.
(32) Ozaki, K.; Lee, R. T.; Lee, Y. C.; Kawasaki, T. *Glycoconjugate J.* **1995,** *122*, 268.
(33) DeFrees, S. A.; Gaeta, F. C. A.; Lin, Y.-Ch.; Ichikawa, Y.; Wong, C.-H. *J. Am. Chem. Soc.* **1993**, *115*, 7549.
(34) DeFrees, S. A.; Kosch, W.; Way, W.; Paulson, J. C.; Sabesan, S.; Halcomb, R. L.; Huang, D.-H.; Ichikawa, Y.; Wong, C.-H. *J. Am. Chem. Soc.* **1995**, *117*, 66.
(35) Lin, C.-H.; Shimazaki, M.; Wong, C.-H.; Koketsu, M.; Junega, L. R.; Kim, M. *Bioorg. Med. Chem* **1995**, *3*, 1625.
(36) Jencks, W. P. *Proc. Natl. Acad. Sci. U.S.A.* **1981**, *78*, 4046.
(37) Jencks, W. P. *Adv. Enzymol.* **1975**, *43*, 219.
(38) Murphy, K. P.; Xie, D.; Thompson, K. S.; Amzel, L. M.; Freire, E. *Proteins: Struct., Fumct., Genet.* **1993**, *18*, 63.
(39) Dunitz, J. D. *Science* **1994**, *264*, 670.
(40) Spolar, R. S.; Record, M. T. *Science* **1994**, *263*, 777.
(41) Starkweather, H. W.; Boyd, R. H. *J. Phys. Chem.* **1960**, *64*, 410.
(42) Gellman, S. H.; Dado, S. P.; Liang, G. P.; Adams, B. *J. Am. Chem. Soc.* **1991**, *113*, 1164.
(43) Yoshiharu, T.; Nose, T.; Hata, T. *Polym. J.* **1974**, *6*, 51.
(44) Page, M. I.; Jencks, W. P. *Proc. Natl. Acad. Sci. U.S.A.* **1971**, *68*, 1678.

ensiformis.[46] The con A monomer has a molecular weight of 26 000 Da and associates into higher order aggregates. In the pH range 5.0−5.6, con A exists exclusively as dimers, while at higher pH the dimers form tetramers; at pH 7.0, tetramer is the predominant form. Succinylation provides a form of the protein that remains dimeric at all pH values. Numerous crystallographic structures of con A to resolutions of 2.0 Å both in native and saccharide-bound forms have been reported.[47−49]

Our multivalent ligands were prepared on a dendritic scaffolding. The synthetic approach is convergent, rather than divergent, allowing glycosidic coupling to the growing polymer at an early stage of the synthesis. We note that our approach also allows total flexibility with regard to the surface composition of polymers displaying two types of functionality, although we have not utilized this facet of the strategy here. The synthesis is based on a benzene-1,3,5-tricarboxylic acid core similar to that devised by Neenan and Miller.[50] In their original synthesis, these researchers formed carboxylic esters at each step and carried a benzylic alcohol as the nucleophile, protected as a silyl ether. Ultimately, the synthesis was limited by difficulties in deprotecting the alcohol nucleophile and acid degradation of the polymer. Our approach replaces ester linkages by amides and carries an amine nucleophile protected as the azide. The enhanced stability of the amide linkage coupled with the facile exposure of the amine nucleophile obviates the limitations of the earlier approach. In principle, the tradeoff for the enhanced stability of the amide relative to the ester is decreased solubility: such limitations were not encountered here.

Synthesis of the dendrimer scaffolding proceeds from benzene-1,3,5-tricarboxylic acid trimethyl ester **1** (Scheme 1). A 76% yield of the monoacid is achieved by hydrolysis with KOH in 18 h. Exclusive production of the monoacid can be achieved by treatment of triester **1** with pig liver esterase. This enzyme, widely utilized as a chiral catalyst in organic synthesis, does not accept charged substrates and cleanly converts triester **1** to monoacid diester **2**. The low solubility of **1** renders enzymatic reaction exceptionally slow: conversion of 9 g of triester with 3000 units of enzyme required 14 days to proceed to completion. As a result, simple base hydrolysis was typically a superior reaction, despite generation of minor byproducts. Selective reduction of monoacid diester **2** was effected with $BH_3 \cdot Me_2S$, and conversion of the resulting benzylic alcohol **3** to the required benzylic azide **5** was completed by sequential treatment with thionyl chloride and sodium azide. Although all the ligands utilized in this study display carbohydrate uniformly on the surface, patterned surfaces displaying two or more classes of functionality may be desirable in other applications. Preparation of such species requires differentiation of the arms of the growing dendrimer, achievable by selective ester cleavage of compound **5**. For this synthesis, both methyl esters were cleaved by KOH to yield the diacid **6**. Finally, the 5-azidomethylbenzene-1,3 dicarboxylate was converted to the diacid chloride with thionyl chloride.

Mannose was coupled to the growing dendrimer through an aminopropanol spacer. α-(Tetra-*O*-acetyl)mannopyranosyl trichloroacetimidate (**8**) was coupled under TMSOTf promotion to 3-azidopropanol to yield **9**. Reduction of the azide preceded coupling to the appropriate acyl chloride in the presence of triethylamine to produce protected mono-, bi-, and trivalent ligands **10**, **12**, and **14** (Scheme 2). Deprotection under Zemplen conditions and purification by silica chromatography yielded ligands **11**, **13**, and **15**, respectively. Alternatively, hydrogenation of protected bivalent ligand **12** followed by coupling to 5-azidomethylbenzene-1,3-dicarboxylate dichloride (**7**) and benzene-1,3,5-tricarbonyl trichloride produced protected tetra- and hexavalent ligands **16** and **18**. Deacetylation under Zemplen conditions and purification by gel permeation chromatography completed the syntheses of the required ligands **17** and **19** (Scheme 3).

Scheme 1[a]

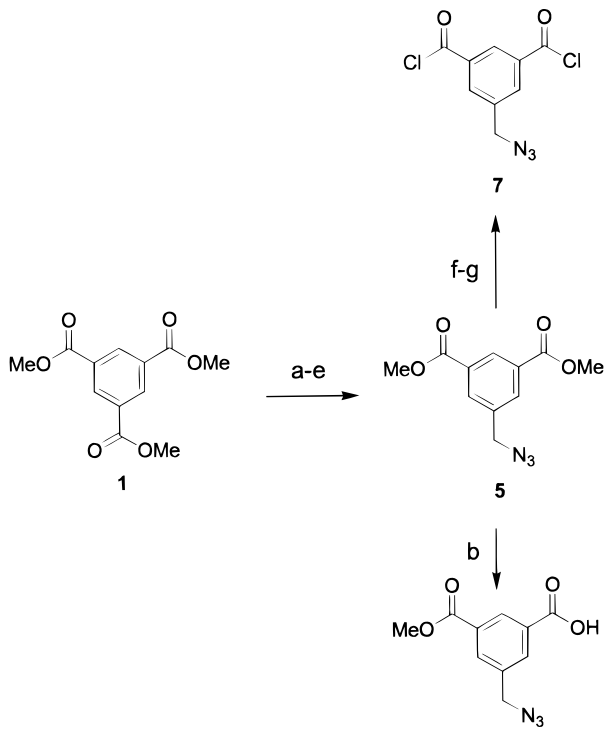

[a] Conditions: (a) H_2SO_4, MeOH, 80 °C; (b) 1.05 equiv of KOH; (c) BMS; (d) $SOCl_2$; (e) NaN_3; (f) 1 M NaOH; (g) $SOCl_2$.

Simple HSEA calculations show a single family of low-energy conformers of the second-generation (tetravalent) ligand. With the two amides of the central ring oriented in a cis/trans orientation, the two dimeric halves extend in a parallel fashion in different planes, minimizing steric interaction. The extended conformation of the second-generation ligand places distal carbonyl carbons some 16 Å apart and separates saccharide residues by 12, 16, and 22 Å (anomeric oxygen to anomeric oxygen), with a maximum possible spacing of roughly 30 Å. The hexavalent structure extends this maximum distance modestly to near 36 Å.

Binding of Concanavalin A to Polyvalent Mannosides. The evaluation of protein−carbohydrate interaction strengths is a nontrivial undertaking. Historically, protein−carbohydrate binding has been evaluated by variations of the Landsteiner hapten inhibition assay. This protocol measures the ability of a soluble saccharide to inhibit the aggregation and precipitation of a polyvalent lectin by a multivalent saccharide ligand. Protein−carbohydrate binding free energies are then assumed to be inversely proportional to IC_{50} values. While the technique offers the advantage of simplicity, the results are both notoriously irreproducible from laboratory to laboratory and difficult to

(45) Mammen, M.; Sakhnovich, E. I.; Whitesides, G. M. *J. Org. Chem.* **1998**, *63*, 3168.
(46) Goldstein, I. J.; Poretz, R. D. In *The Lectins: Properties, Functions, and Applications in Biology and Medicine*; Liener, I. E., Sharon, N., Goldstein, I. J., Eds.; Academic: New York, 1986.
(47) Naismith, J. H.; Field R. A. *J. Biol. Chem.* **1996**, *271*, 972.
(48) Naismith, J. H.; Emmerich, C.; Habash, J.; Harrop, S. J.; Helliwell, J. R.; Hunter, W. N.; Raftery, J.; Kalb, A. J.; Yariv, J. J. *Acta Crystallogr.* **1994**, *D50*, 847.
(49) Moothoo, D. N.; Naismith, J. H. *Glycobiology* **1998,** *8*, 173
(50) Miller, T. M.; Kwock, E. W.; Neenan, T. X. *Macromolecules* **1992**, *25*, 5, 3143.

Scheme 2

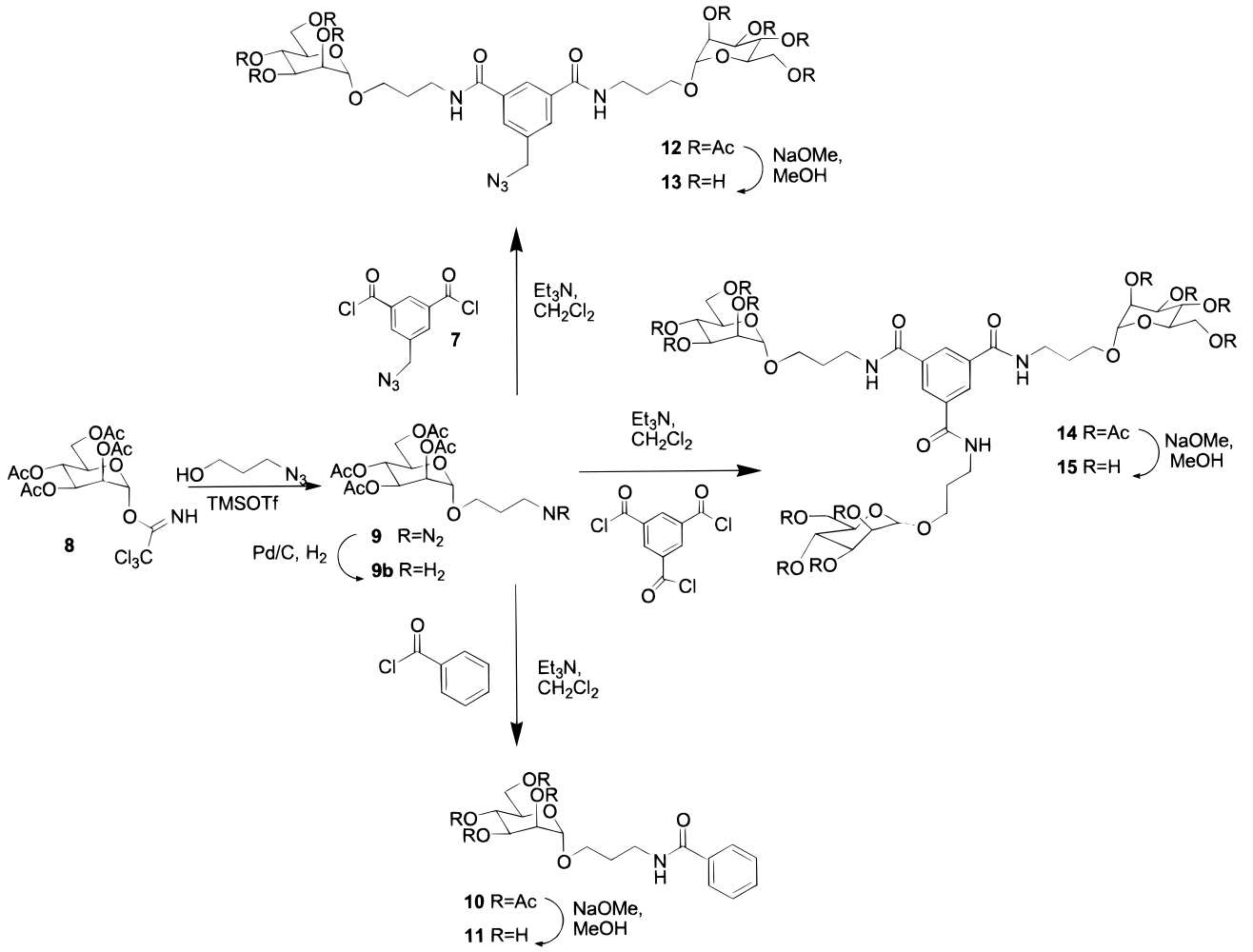

interpret at a molecular level. More recently, titration microcalorimetry has been utilized to study protein−carbohydrate interaction.[51−60] In this technique, a soluble protein is titrated with aliquots of a soluble ligand. The heat evolved during ligand addition serves as a reporter signal for binding that is deconvoluted to yield a binding constant, in turn relatable to the free energy of binding. The technique also evaluates binding enthalpies directly: this measure, in conjunction with the free energy of binding, provides an entropy of binding. Evaluation of ΔH as a function of temperature yields the change in molar heat capacity accompanying binding, ΔC_p, which in turn allows dissection of both binding enthalpies and entropies into contributions arising from specific molecular events.[61−64]

Table 1. Binding of Dendtritic Ligands to Concanavalin A Calorimetry[a] Agglutination

ligand	K_{eq} (M^{-1})	N[b]	ΔG[c]	ΔH[c]	$T\Delta S$[c]	IC_{50} (μM)	potency[d]
Me α-Man	7 700	1	−5.3	−6.8	−1.5	520	1
11	11 820	1	−5.5	−6.4	−0.9	280	2
13	18 782	1	−5.8	−8.9	−3.1	380	1.4
15	3 734	0.8	−4.9	−8.6	−3.7	630	0.8
17	9 640	1	−5.4	−4.9	+0.5	17	31
19	7 504	1	−5.3	−3.8	+1.5	41	13

[a] All calorimetric values are in terms of mannose equivalents. [b] Stoichiometry of binding, carbohydrate:protein. [c] In kcal mol^{-1} at 298 K. [d] Values corrected for valency and expressed relative to methyl α-D-mannopyranoside.

The bindings of mono-, di-, tri-, tetra-, and hexavalent ligands **11**, **13**, **15**, **17**, and **19** to dimeric concanavalin A were evaluated by both titration microcalorimetry and hemagglutination assay (Table 1). By agglutination assay, *tetra- and hexavalent ligands demonstrate significant cluster glycoside effects*. As has been previously observed, the magnitude of the effect depends exquisitely on the size and shape of the ligands. Thus, while no multivalency effect is observed for bi- or trivalent ligands, tetra- and hexavalent ligands show cluster glycoside effects of 30- and 17-fold, respectively.

Calorimetric evaluation of binding provides a markedly different picture. Titration microcalorimetry of all multivalent

(51) Williams, B. A.; Chervenak, M. C.; Toone, E. J. *J. Biol. Chem.* **1992**, *267*, 22907.
(52) Weatherman, R. V.; Hortell, K. H.; Chervenak, M. C.; Kiessling, L. L.; Toone, E. J. *Biochemistry* **1996**, *35*, 9−3624.
(53) Chervenak, M. C.; Toone, E. J. *Bioorg. Med. Chem.* **1996**, *4*, 1963−1977.
(54) Gupta, D.; Cho, M.; Cummings, R. D.; Brewer, C. F. *Biochemistry* **1996**, *35*, 15236.
(55) Mandal, D. K.; Bhattacharyya, L.; Koenig, S. H.; Brown, R. D., III; Oscarson, S.; Brewer, C. F. *Biochemistry* **1994**, *33*, 1157.
(56) Sigurskjold, B. W.; Bundle, D. R. *J. Biol. Chem.* **1992**, *267*, 8371.
(57) Sigurskjold, B. W.; Altman, E.; Bundle, D. R. *Eur. J. Biochem.* **1991**, *197*, 239.
(58) Schwarz, F. P.; Puri, K. D.; Bhat, R. G.; Surolia, A. *J. Biol. Chem.* **1993**, *268*, 7668.
(59) Schwarz, F. P.; Puri, K.; Surolia, A. *J. Biol. Chem.* **1991**, *266*, 24344.
(60) Bains, G.; Lee, R. T.; Freire, E. *Biochemistry* **1992**, *31*, 12624.
(61) Chervenak, M. C.; Toone, E. J. *J. Am. Chem. Soc*, **1994**, *116*, 10533
(62) Isbister, B. D.; St. Hilaire, P. M.; Toone, E. J. *J. Am. Chem. Soc.* **1995**, *117*, 12877.
(63) Oas, T. G.; Toone, E. J. *Adv. Biophys. Chem.* **1997**, *6*, 1.
(64) Chervenak, M. C.; Toone, E. J. *Biochemistry* **1995**, *34*, 5685.

Scheme 3

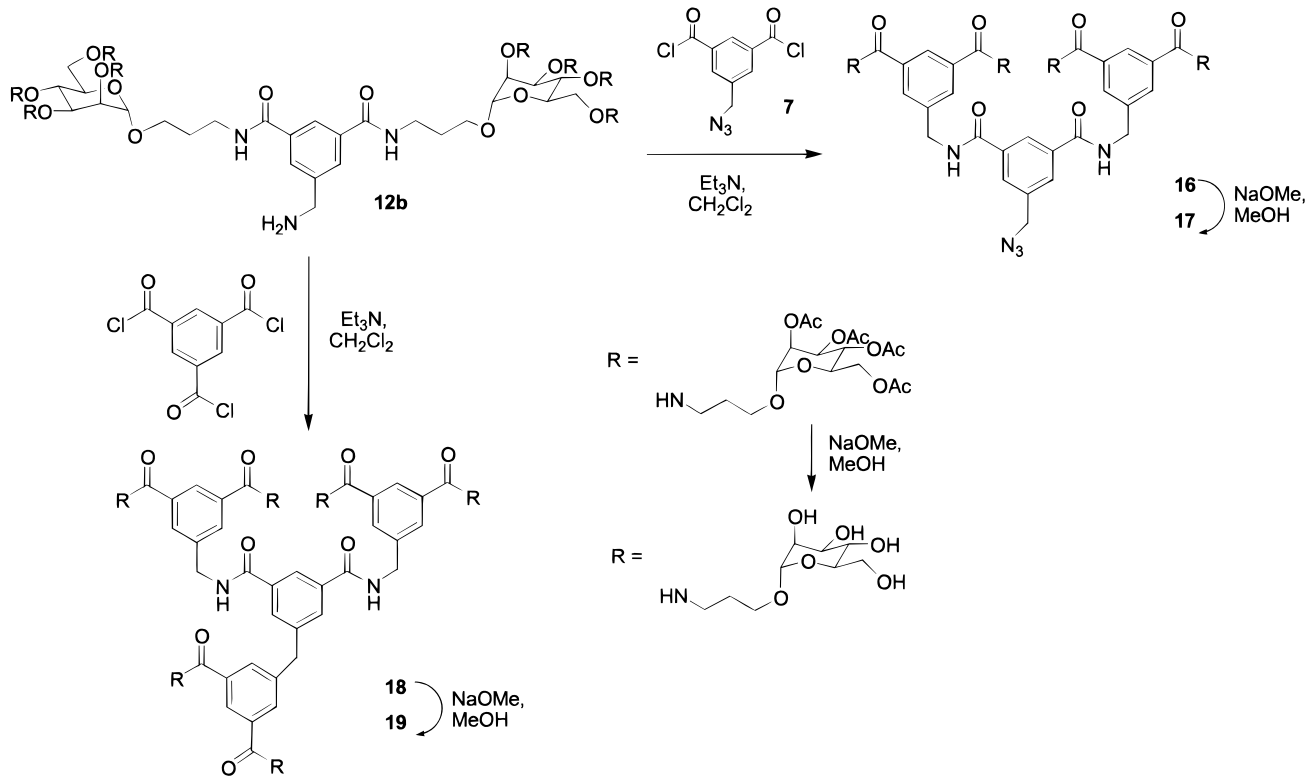

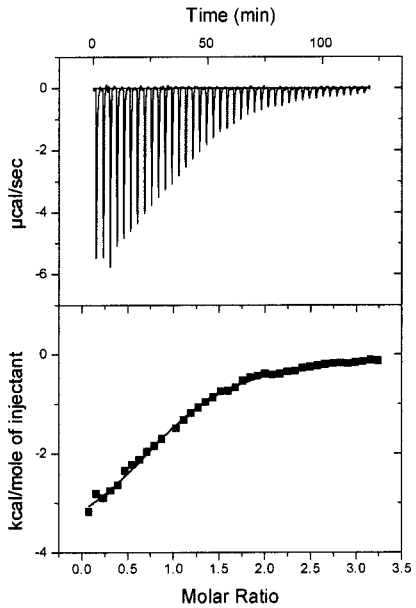

Figure 1. Calorimetric data for titration of concanavalin A, 0.51 mM, with hexavalent ligand **19**, 24.9 mM. Both protein and ligand were dissolved in buffer conisisting of 50 mM dimethylglutarate, 250 mM NaCl, 1 mM $CaCl_2$, and 1 mM $MnCl_2$ adjusted to pH 5.2. Top, raw (power vs time) data; bottom, integrated heat vs molar ratio of ligand. Solid line shows best fit of data using a one-site model: $n = 0.96 \pm 0.02$; $K = 6900 \pm 500$; $\Delta H = -4.0 \pm 0.1$ kcal/mol; $\chi^2 = 14$. A fit to a two-site model does not provide a statistically superior fit.

ligands yields curves indicative of simple reversible binding (Figure 1). This behavior is somewhat surprising, given that multivalent ligands aggregate and precipitate multivalent lectins. Indeed, examination of the contents of the calorimeter cell following all titrations showed evidence of aggregation; typically solutions were cloudy. This aggregation is apparently not reported by the calorimetric experiment, at least with respect

Scheme 4

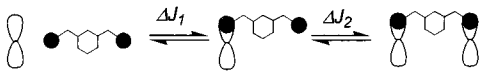

to curve shape. An irreversible aggregation subsequent to, i.e., coupled with, ligand binding would make the *apparent* protein−carbohydrate binding constant infinite and result in a square curve. If aggregation/irreversible precipitation was slow on the titration time scale, the value *c*, which in turn determines the curve shape, would vary continuously during the titration, producing a curve that could not be deconvoluted for a single value of K_{eq}. Apparently then, aggregation/precipitation does not remove a significant amount of protein from solution during the course of calorimetric titration.

The thermodynamics of multivalent ligand binding provide insights into the physical processes evaluated by calorimetry and hemagglutination. Table 1 reports values of binding free energies, enthalpies, and entropies averaged over the total number of monosaccharides in each multivalent ligand. The narrow range of binding free energies provides binding curves that are well fit by a single site model, despite the wide disparity in observed binding enthalpies. It is possible to separate the contributions of individual microscopic binding events of a multivalent ligand to the reported average value. Consider binding of the bivalent ligand **13** (Scheme 4). The observed thermodynamic parameters are the averages of the two microscopic constants ΔJ_1 and ΔJ_2, where ΔJ represents the change in enthalpy, entropy, free energy, or heat capacity accompanying binding. By assuming ΔJ_1 is equivalent to that of the monovalent ligand **11**, the values of ΔJ_2 are accessible. Similarly, microscopic thermodynamic constants for the tetra- and hexavalent ligands can be extracted.[65] Here, absent discrete values for ΔJ_3

(65) Because thermodynamic parameters are state functions, the order of binding does not affect this analysis; we do not imply any particular kinetic progression of binding of any of the multivalent ligands.

Table 2. Thermodynamic Parameters for the Binding of Successive Saccharide Moieties of Multivalent Ligands **11**, **13**, **15**, **17**, and **19**

binding of ligand	ΔG	ΔH	$T\Delta S$
1	−5.5	−6.4	−0.9
2	−6.1	−11.4	−5.3
3/4	−5.0	−0.9	+4.1
5/6	−5.1	−1.6	+3.5

and ΔJ_5, we can obtain only average values for $\Delta J_3/\Delta J_4$ and for $\Delta J_5/\Delta J_6$. The values for each set of microscopic constants are shown in Table 2.

An even cursory examination of the data shows an immediate and obvious trend*: IC_{50} values correlate with calorimetrically derived entropies of ligand binding (i.e., negatively with enthalpies of ligand binding) but not free energies of ligand binding*. It is difficult to unambiguously assign a physical basis for this observation; two processes might reasonably result in the observed thermodynamic pattern. First, aggregation could alter the thermodynamics of protein−carbohydrate binding but in a compensating fashion. A reduction in favorable binding enthalpy would be accompanied by an increase in favorable entropy of binding. While such compensating events have been observed for a wide range of interacting systems and are indeed almost a hallmark of association events in aqueous solution, a physical explanation for such compensating behavior is not obvious.[66] Furthermore, a number of previously reported enthalpy−entropy compensation events were subsequently shown to be the result of correlated errors; Grunwald has written on the dangers of invoking compensation arguments in the absence of a clear mechanistic rationale for doing so.[67] Thus, while such an explanation cannot be ruled out, the prescription of Occam's razor makes a compensation argument unattractive. Alternatively, an aggregation process, either following or concomitant with ligand binding and typified by a large positive enthalpy, would produce the observed pattern of enthalpy−entropy compensation; the enthalpy of aggregation masks a portion of the enthalpy of protein−carbohydrate binding. Because of the experimental design, the free energy change for the aggregation process is not reported, provided it does not alter the free energy of protein−carbohydrate binding. A simple linear correlation between IC_{50} and $\Delta H/\Delta S$ is not immediately apparent because a quantitative estimate of the extent of aggregation is unavailable.

To assess the validity of our hypothesis, dynamic light scattering experiments were performed. At pH 7.0 in the presence of tetravalent ligand, 0.2 mM succinyl concanavalin A showed an apparent molecular weight of 4−6 MDa. In the presence of hexavalent ligand, the apparent molecular weight rises to 6−8 MDa; in both instances the profile is broad, indicative of a range of species. We note parenthetically that examination of succinyl concanavalin A without added ligand yielded results similar to those obtained with native unmodified protein, which shows a hydrodynamic radius of 4 nm and an apparent molecular weight of 100 kDa. This result is at odds with other solution studies that the succinylated protein is dimeric and emphasizes the caution with which solution studies must be treated. Together, these observations suggest that the behavior of polyvalent ligands is more complicated than previously appreciated. Under all circumstances, a range of oligomeric species is present, and the detailed structure of the aggregate depends on the precise experimental conditions.

(66) Lumry, R.; Rajender, S. *Biopolymers* **1970**, *9*, 1125.

(67) Grunwald, E.; Comeford, L. L. In *Protein−Solvent Interact*; Gregory, R., Ed.; Dekker: New York, 1995; pp 421−43.

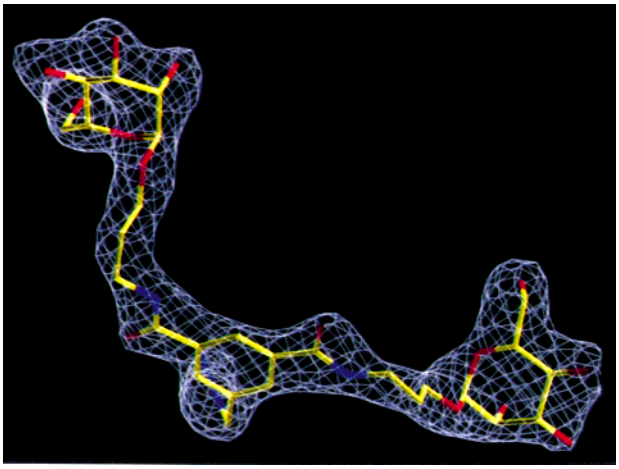

Figure 2. Quality of the data. The $F_o - F_c$ difference electron density map is calculated with phases from a model that had never included the bivalent ligand. The bivlaent ligand is shown in stick form in its final refined position (red, oxygen; blue, nitrogen; yellow, carbon). Hydrogen atoms are not included in the figure. The map (blue wire) is contoured at 3σ above the mean.

Assuming the observed enthalpy−entropy compensation results from an endothermic, entropically driven aggregation process masking the enthalpy of protein−carbohydrate binding, the negative correlation between agglutination IC_{50} values and the apparent enthalpy of ligand binding suggests that the agglutination assay *does not evaluate the strength of protein−carbohydrate binding*. Rather, this assay measures the ability of a polyvalent saccharide ligand to drive aggregation processes. Accordingly, all "binding" constants obtained by hemagglutination should be regarded cautiously. Interpretation of agglutination results in terms of protein−carbohydrate affinity is not warranted in light of the results presented here: 30-fold variation in IC_{50} values are observed with *no* change in protein−carbohydrate affinity. We note that this caution is not to suggest that IC_{50} results are not of use in the study of protein−carbohydrate interaction. Indeed, in many respects hemagglutination studies are a far more relevant measure of *activity* than are assays designed exclusively to evaluate protein−carbohydrate binding. It is clear, however, that attempts to interpret agglutination data in terms of affinity, in the normal sense of the term, can be dangerously misleading.

We note additionally that calorimetry is not the only experimental technique capable of observing the discrepancies we have noted here; indeed, any technique that exclusively observes protein−carbohydrate binding uncoupled to subsequent aggregation and precipitation events should report values identical to those reported in Table 1. Such techniques, including NMR and fluorescence titrations, have previously been utilized for the assay of protein−carbohydrate affinity, although not with multivalent ligands. Kiessling and co-workers recently reported evaluation of the binding of a series of multivalent mannosides to concanavalin A using surface plasmon resonance.[68] In these studies, enhancements in affinity observed for high-valent ligands in agglutination assays were greatly reduced in precipitin assays but were still observed. The longest of these ligands are capable of spanning two sites, although enhancements in activity are observed for compounds of lesser lengths. Whether the ligands used in the Kiessling study will continue to show enhanced affinity in other assays, such as those used here, is unclear.

(68) Mann, D. A.; Dannai, M.; Maly, D. J.; Kiessling, L. L. *J. Am. Chem. Soc*. **1998**, *120*, 10370.

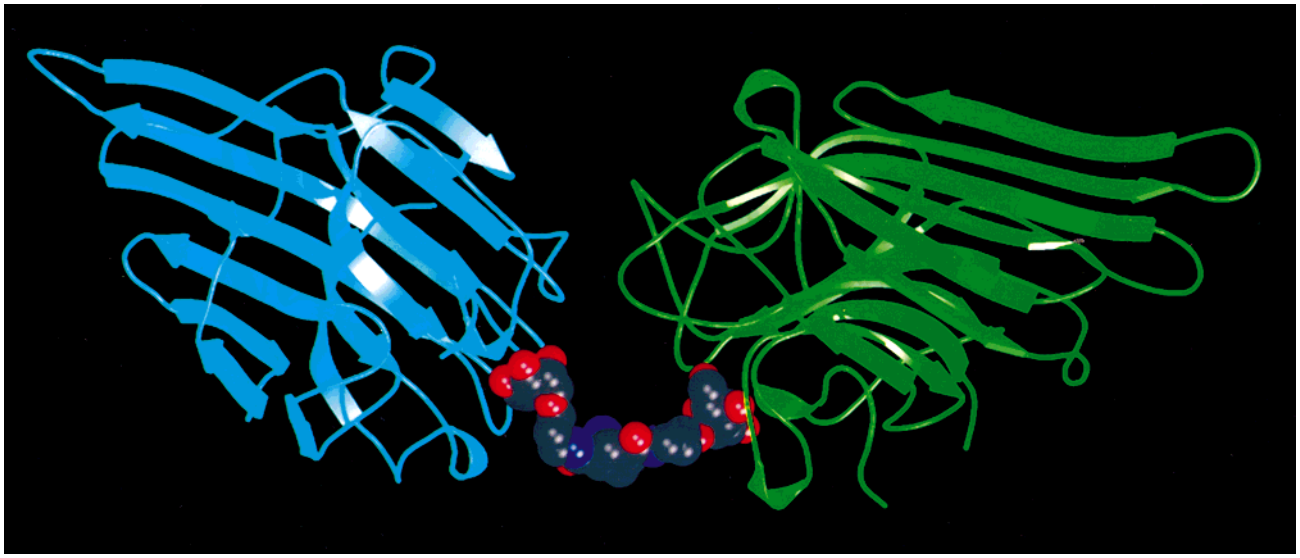

Figure 3. Cross-link between concanavalin A monomers. The monomers are shown as backbone traces (red and blue) and the ligand in a space-filling representation (atomic color scheme as in Figure 3). Both the extended conformation of the ligand and the cis/trans orientation about the amide linkages are obvious. Cross-linked protein monomers do not make substantial contact with each other.

Structure of Concanavalin A−Polyvalent Ligand Complexes. Aggregation and precipitation effects uniformly preclude X-ray analysis of polyvalent protein−carbohydrate complexes. In an attempt to circumvent this limitation, we cocrystallized succinyl concanavalin A with ligands **13**, **15**, **17**, and **19**. Although it is well known that succinylation results in dimeric protein at all pH values, no crystal structure of this derivative has been reported. Remarkably, cocrystals of all four ligands were obtained. To date, we have diffracted cocrystals of bivalent and trivalent ligands. Details of the crystallization, data collection, and molecular replacement have been reported elsewhere.[69] The divalent complex has space group $C222_1$, with cell dimensions $a = 99.1$ Å, $b = 127.4$ Å, $c = 118.9$ Å, and diffracts to 2.66 Å. The crystallographic asymmetric unit contains a dimer (68% solvent). Overall anisotropic thermal parameter and bulk solvent corrections were applied to the data using standard CNS protocols for refinement.[70] The starting *R*-free was 32% for all data between 26 and 2.66 Å. Restrained refinement of positional and thermal parameters with CNS reduced the *R*-free to 25%. Noncrystallographic restrains were applied to thermal and positional parameters throughout the refinement. At this stage, clear density was visible for the ligand (Figure 3) and metal ions ($2Mn^{2+}$ and $2Ca^{2+}$). These were included in the model and refinement continued.

In both instances, concanavalin A crystallizes in tetrameric form *despite succinylation*: apparently, crystal packing forces compensate for the repulsive interactions introduced by succinylation. Clear density could be seen for a succinyl group on Lys 101 in one monomer and was included in the model. Density for Lys 101 in the other monomer was visible but not clear enough to build a model of the succinyl group. No other succinyl groups were visible, raising the issue of a molecular mechanism for inhibition of tetramerization by protein derivatization. Presumably, other lysine residues are incompletely succinylated: in aggregate these acylations disfavor dimer dimerization.

The supramolecular structure consists of infinite plates extending in two dimensions and cross-linked by bivalent ligands (Figure 4). The structure also allows crystallographic examination of a saccharide-containing dendron, the first such structure of which we are aware. The ligand geometry was defined using the Engh and Huber compendium of bond distances.[71] Statistics on the final refined model are given in Table 3. The absolute value of *R*-free (20%) is probably artificially low due to noncrystallographic symmetry; however, the trend (decrease upon refinement) validates our refinement protocol. The loop between residues 118 and 122 is disordered in this structure, as in all other con A structures. As expected, the core of the dendrimer structure exists in a planar arrangement. The amides are arranged in a cis/trans orientation, providing a pseudo-*C*2 axis of symmetry between the two saccharide residues. Both saccharides occupy concanavalin A binding sites in identical fashions, essentially as the monosaccharide (Figure 2). In both instances, the linker aglycon is oriented in a −60° conformer, in accordance with the general observation that carbohydrates are bound by lectins at or near their HSEA minimum energy conformation.[10] The final coordinates and structure factors have been deposited with the Protein Data Bank (PDB coordinate entry 1qgl).[72]

The trivalent complex has the same space group and very similar cell dimensions: $a = 99.4$ Å, $b = 127.2$ Å, $c = 118.7$ Å. A full data set to 3.0 Å was collected on the trivalent ligand con A complex. Molecular replacement and refinement proceeded in a manner identical to that described for the divalent complex above. However, no density was visible for the third sugar, and as all the monosaccharide binding sites of con A in the crystal are occupied, we concluded that this part of the ligand is disordered. In conjunction with the observation of a less than 1:1 stoichiometry during calorimetric experiments, this observation raises the possibility that the soluble aggregates formed in solution pack in a fashion similar to the insoluble aggregates observed during diffraction. Binding of only two carbohydrates of a trivalent ligand would give rise to a binding stoichiometry of 0.67. The value of 0.8 observed here suggests that the aggregates are likely of lower order than the crystal form. Nonetheless, the low stoichiometry is most reasonably inter-

(69) Moothoo, D. N.; McMahon, S. M.; Dimick, S. M.; Toone, E. J.; Naismith, J. H. *Acta Crystallogr.* **1998**, *D54*, 1023.

(70) Adams, P. D.; Pannu, N. S.; Read, R. J.; Brunger, A. T. *Proc. Natl. Acad. Sci. U.S.A.* **1997**, *94*, 5018.

(71) Engh, R. A.; Huber, R. *Acta Crystallogr.* **1991**, *A47*, 392.

(72) Bernstein, F. C.; Koetzle, T. F.; Williams, G. J. B.; Myer, E. F., Jr.; Brice, M. D.; Rodgers, J. R.; Kennard, O.; Shimanouchi, T.; Tasumi, M. *J. Biol. Chem.* **1977**, *112*, 535.

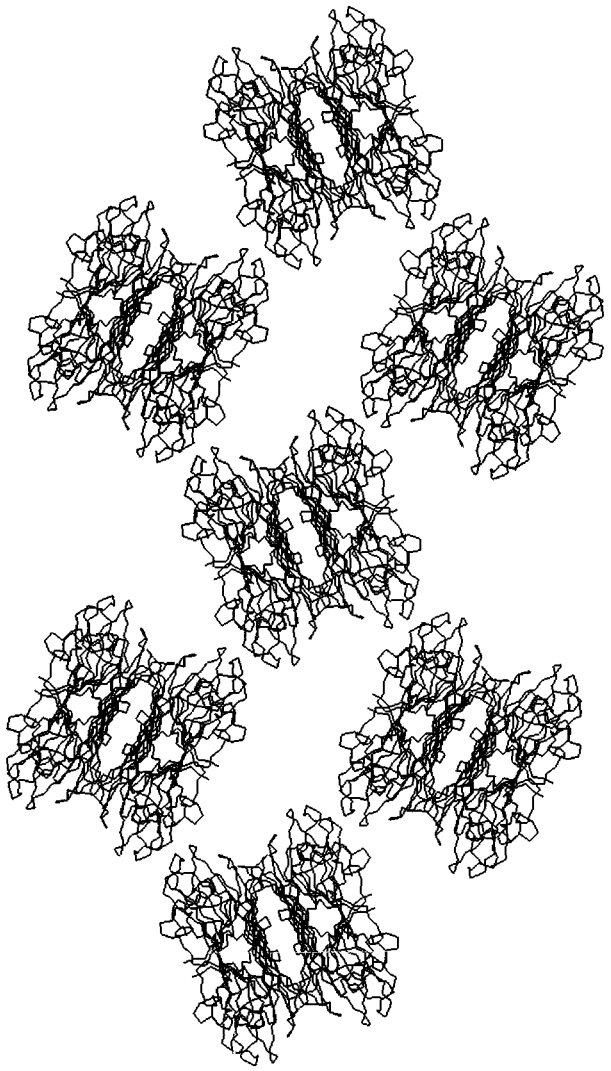

Figure 4. Crystal packing arrangement of the complex. Concanavalin A is represented in a backbone trace. The cross-linking ligands have been omitted for clarity. The standard con A tetramer is clearly visible and forms an infinite two-dimensional array via the cross-linking ligands. The crystal is formed of offset stacks of two-dimensional arrays.

preted in terms of some form of local order in aggregate formation that precludes binding of the third saccharide of a trivalent ligand, even in solution.

The conclusions of the work presented here are clear. A range of species is formed when multivalent ligands are bound to multivalent lectins, provided the lectins orient binding sites in several directions and are capable of forming cross-links. Those observations of high "affinity" of multivalent glycoconjugates rather reflect the propensity of such ligands to form aggregates, as opposed to any enhancement in actual protein−carbohydrate affinity. Finally, IC_{50} values from agglutination assays correlate with entropies—not free energies—of ligand binding; agglutination assays should not be considered as a measure of protein−carbohydrate affinity. We continue our studies on the role of multivalency in protein−carbohydrate interaction and will report our results in due course.

Experimental Section

General. D-Mannose (lot no. 05115CG), benzenetricarboxylic acid, and benzene-1,3,5-tricarbonyl trichloride were purchased from Aldrich Chemical and used without further purification. Dichloromethane was distilled from calcium hydride. THF was distilled from sodium/benzophenone ketyl. All other chemicals were reagent grade and used without further purification. Column chromatography was performed with flash grade silica gel. Thin-layer chromatography plates were Silica Gel 60 F_{254} (Merck) and visualized with Hanessian stain. ^{1}H NMR spectra were recorded on a GE QE-300, Varian 500, or Varian 600 instrument operating at 300.150, 500.137, or 599.892 MHz, respectively, in either $CDCl_3$ or D_2O referenced to TMS or TSP at 0 ppm, respectively. ^{13}C NMR spectra were recorded on a GE QE-300 or Varian 600 instrument operating at 75.48 or 150.86 MHz, respectively, in $CDCl_3$ referenced to $CDCl_3$ at 77.0 ppm. Mass spectrometry was performed on a JEOL JMS-SX102A instrument.

Table 3. Crystallographic Data Collection Statistics and Refinement Statistics

no. of unique reflections	21 182
completeness of data (%) (26.0−2.66 Å/2.75−2.66 Å)	96.4/98.3
R_{merge}[a] (I) (%) (26.0−2.66/2.75−2.66)	7.2/20.7
average data redundancy (26.0−2.66 Å/2.75−2.66 Å)	2.5/2.2
% of data > 1σ (26.0−2.6 Å/2.75−2.66 Å)	94/83
refinement	
resolution range (Å)	26−2.66
R-free[b] % (uncorrected)[c]	20.0 (25.7)
R-factor % (uncorrected)	17.6 (23.9)
bond rms deviation (Å)[d]	0.008
angle rms deviation (deg)[d]	1.70
noncrystallographic symmetry rms deviation (C_α atoms) (Å)	0.10
B-factor bonded atoms rms deviation (Å^2)[e]	1.75
Ramachandran core/additional (%)[f]	86.7/12.8
average B-factor (Å^2)	28.9
no. of ordered protein atoms	3624
no. of solvent molecules	72
total no. of ordered non-hydrogen atoms	3625

[a] $R_{merge(I)} = S_{hkl}S_i|I_i - I(hkl)|/S_{hkl}S_iI_i(hkl)$. [b] R-free is the crystallographic residual calculated on 10% of data excluded during refinement. [c] Uncorrected is without CNS anisotropic and bulk solvent corrections. [d] Root-mean-square deviation from Engh and Huber ideal values.[71] [e] Calculated with MOLEMAN (G. J. Kleywegt, unpublished program). [f] Core and additionally allowed regions as defined by PROCHECK.[70] One disordered residue is in a generously allowed region, and no residues are in disallowed regions.

Synthesis of Ligands. Trimethyl 1,3,5-Benzenetricarboxylate (1). Benzenetricarboxylic acid (8.0 g, 38 mmol) was dissolved in methanol (140 mL). Concentrated sulfuric acid (2 mL) was added. The solution was refluxed for 24 h. Solvent was removed under reduced pressure, the residue was dissolved in chloroform (150 mL) and washed with saturated bicarbonate (200 mL), and the solvent was removed under reduced pressure to give the desired product **1** as a white powder (9.15 g, 95%): mp 144−144.5 °C (ref 145−147 °C). ^{1}H and ^{13}C NMR spectra were identical to those previously reported.[73]

Dimethyl 1,3,5-Benzenetricarboxylate (2). Trimethyl 1,3,5-benzenetricarboxylate (1.11 g, 4.40 mmol) was dispersed in MeOH (100 mL). Aqueous NaOH (3.93 mL of 1.0 M, 3.93 mmol, 0.9 equiv) was added. The suspension was stirred vigorously and slowly dissolved during 8 h. After 18 h, solvent was removed under reduced pressure. Dichloromethane (75 mL) was added. The organic phase was washed with saturated $NaHCO_3$ (2 × 75 mL), dried ($MgSO_4$), and evaporated to give unreacted starting material (260 mg, 23%). The aqueous washes were acidified (pH 2.0) with concentrated HCl, yielding a milky white suspension that was washed with ethyl acetate (2 × 75 mL). The combined organic phases were washed with brine (1 × 30 mL) and dried ($MgSO_4$), and the solvent removed to give a **2** as a white powder (800 mg, 76%): ^{1}H NMR (300 MHz, $CDCl_3$) δ 8.91 (s, 2H), 8.90 (s, 1H), 3.99 (s, 6H) ppm; ^{13}C NMR (75 MHz, $CDCl_3$) δ 169.9, 165.3, 135.2, 135.0, 132.4, 130.4, 52.8 ppm; IR (KBr pellet) ν 3284 (broad), 1735, 1697 cm^{-1}.

Dimethyl 5-Hydroxymethylbenzene-1,3-dicarboxylate (3). 1,3-Dimethylbenzene-1,3,5-tricarboxylate (3.40 g, 14.3 mmol) was dissolved in dry THF (24 mL). Borane−methyl sulfide complex (14.3 mL of 2 M solution in THF, 28.6 mmol) was added slowly,

(73) *Aldrich Library of Fourier Transform NMR*; Aldrich Chemical Co.: Milwaukee, WI, 1989; Vol. 2, 1282C.

accompanied by effervescence. After 24 h of stirring at 27 °C, methanol (50 mL) was added. The solution was stirred at 27 °C for 30 min and concentrated under reduced pressure. The resulting white solid was dissolved in ethyl acetate (75 mL) and washed with water (75 mL), saturated $NaHCO_3$ (75 mL), and brine (50 mL). Solvent was removed under reduced pressure, and the crude product was purified by silica chromatography (PE:EA 3:2) to give **3** as a white solid (2.82 g, 88%): mp 104 °C; ^{1}H NMR (300 MHz, $CDCl_3$) δ 8.58 (t, 1H, J = 1.5 Hz), 8.23 (t, 2H, J = 0.8 Hz), 4.81 (d, 2H, J = 5.9 Hz), 3.95 (s, 6H), 2.20 (t, 1H, J = 5.9 Hz) ppm; ^{13}C NMR (75 MHz, $CDCl_3$) δ 166.2, 141.9, 132.0, 130.8, 129.8, 64.2, 52.2 ppm; IR (KBr pellet) ν 3446 (broad), 1723 cm^{-1}.

Dimethyl 5-Chloromethyl-1,3-benzenedicarboxylate (4). To dimethyl 5-hydroxymethylbenzene-1,3-dicarboxylate (2.0 g, 8.9 mmol) was added $SOCl_2$ (1.3 mL). The solution was refluxed under an argon atmosphere for 1 h. $CHCl_3$ was added to the solution, and the organic phase was washed with 0.1 M NaOH (2 × 50 mL) and brine (50 mL). Solvent was removed under reduced pressure to yield **4** as a white powder (2.0 g, 93%): mp 119−120 °C; ^{1}H NMR (300 MHz, $CDCl_3$) δ 8.62 (t, 1H, J = 1.9 Hz), 8.25 (d, 2H, J = 1.9 Hz), 4.66 (s, 2H), 3.96 (s, 6H) ppm; ^{13}C NMR (75 MHz, $CDCl_3$) δ 165.6, 138.6, 133.7, 131.1, 129.8, 52.3, 44.8 ppm; IR (KBr pellet) ν 1725 cm^{-1}.

Dimethyl 5-Azidomethylbenzene-1,3-dicarboxylate (5). Dimethyl 5-chloromethylbenzene-1,3-dicarboxylate (2.0 g, 8.2 mmol) was dissolved in acetone (30 mL) and water (10 mL). NaN_3 (3.21 g, 49.3 mmol, 6 equiv) was added, and the solution was refluxed for 16 h. Solvent was removed in vacuo, and the residue was dissolved in $CHCl_3$ (75 mL). The organic phase was washed with water (3 × 75 mL) and brine (50 mL). Solvent was removed under reduced pressure to yield **5** as a pale yellow powder (1.99 g, 97%): mp 74−75 °C; ^{1}H NMR (300 MHz, $CDCl_3$) δ 8.65 (t, 1H, J = 1.5 Hz), 8.20 (d, 2H, J = 1.5 Hz), 4.49 (s, 2H), 3.97 (s, 6H) ppm; ^{13}C NMR (75 MHz, $CDCl_3$) δ 165.1, 135.9, 132.7, 132.3, 130.5, 53.2, 51.9 ppm; IR (KBr pellet) ν 2107, 1722 cm^{-1}.

5-Azidomethylbenzene-1,3-dicarboxylate (6). Dimethyl 5-azidomethylbenzene-1,3-dicarboxylate (0.77 g, 3.1 mmol) was dissolved in 1 M methanolic KOH (25 mL), and the resulting solution was refluxed for 1 h. Solvent was removed under reduced pressure, and the residue was dissolved in water (75 mL) and acidified with concentrated HCl to pH 2 to give a milky suspension. The suspension was extracted with ethyl acetate (3 × 50 mL), and the combined organic washes were reduced to yield **6** as a white powder (0.68 g, 99%): mp 212−214 °C; ^{1}H NMR (300 MHz, acetone-d_6) δ 8.52 (t, 1H, J = 1.6 Hz), 8.15 (d, 2H, J = 1.6 Hz), 4.59 (s, 2H) ppm; ^{13}C NMR (75 MHz, acetone-d_6) δ 165.9, 137.5, 133.2, 131.8, 130.1, 53.3 ppm; IR (KBr pellet) ν 2105, 1702 cm^{-1}.

5-Azidomethylbenzene-1,3-dicarbonyl Dichloride (7). 5-Azidomethylbenzene-1,3-dicarboxylate (0.2 g, 0.9 mmol) was dissolved in 1 mL of $SOCl_2$ and refluxed for 1 h. Excess thionyl chloride was removed under reduced pressure to yield **7** as a yellow oil (0.233 g, 100%): ^{1}H NMR (300 MHz, $CDCl_3$) δ 8.77 (s, 1H), 8.35 (s, 2H), 4.62 (s, 2H) ppm; ^{13}C NMR (75 MHz, $CDCl_3$) δ 166.9, 138.6, 135.8, 134.9, 133.2, 53.2 ppm; IR (neat) ν 2108, 1762 cm^{-1}.

3-Azidopropyl 2,3,4,6-Tetra-*O*-acetyl-α-D-mannopyranoside (9). 2,3,4,6-Tetra-*O*-acetyl-α-D-mannopyranosyl trichloroacetimidate **8** (930 mg, 1.9 mmol) was dissolved in CH_2Cl_2 (10 mL) with 4-Å powdered molecular sieves (1 g). 3-Azidopropanol (948 mg, 9.5 mmol, 5 equiv) was added, and the reaction mixture was chilled to −30 °C. After the mixture was stirred for 30 min, TMSOTf (155 μL, 0.75 mmol, 0.4 equiv) was added during 5 min. The reaction mixture was stirred and allowed to warm to 0 °C during 4 h, at which time TLC (4:1 light petroleum ether:ethyl acetate) showed complete disappearance of starting material. Solid $NaHCO_3$ (250 mg) was added, and the reaction mixture was stirred for 10 min. The mixture was filtered over Celite and concentrated. The crude material was purified by flash chromatography over silica (5:1 light petroleum ether:ethyl acetate) to yield **9** as a viscous, colorless oil (680 mg, 81%): ^{1}H NMR (300 MHz, $CDCl_3$) δ 1.77−1.88 (m, 2H, $OCH_2CH_2CH_2N_3$), 1.96 (s, 3H, −OCOCH_3), 2.02 (s, 3H, −OCOCH_3), 2.08 (s, 3H, −OCOCH_3), 2.13 (s, 3H, −OCOCH_3), 3.42 (t, 2H, J = 6.4 Hz, $OCH_2CH_2CH_2N_3$), 3.48−3.51 (m, 1H, −OCH_2-$CH_2CH_2N_3$), 3.72−3.79 (m, 1H, −OC$H_2CH_2CH_2N_3$), 3.80−3.93 (m, 1H), 4.06−4.10 (dd, 1 H, J = 2.4, 12.2 Hz), 4.22−4.28 (dd, 1H, J = 5.4, 12.2 Hz), 4.79 (d, 1H, H-1, J = 1.4 Hz), 5.20−5.28 (m, 3H) ppm; ^{13}C NMR (75.48 MHz, $CDCl_3$) δ 20.00 (OCOCH_3), 20.19 (OCOCH_3), 27.89 ($OCH_2CH_2CH_2N_3$), 47.35 ($OCH_2CH_2CH_2N_3$), 61.75, 64.11 ($OCH_2CH_2CH_2N_3$), 65.35, 67.89, 68.30, 68.74, 96.89 (C-1), 169.04 (OCOCH$_3$), 169.23 (OCOCH$_3$), 169.37 (OCOCH$_3$), 169.95 (OCOCH$_3$) ppm; IR (neat) ν 2955, 2257, 2098, 1751, 1370, 1239, 913, 739, 648 cm^{-1}.

3-(Benzylamido)propyl 2,3,4,6-Tetra-*O*-acetyl-α-D-mannopyranoside (10). 3-Azidopropyl 2,3,4,6-tetra-*O*-acetyl-α-D-mannopyranoside (95 mg, 0.22 mmol) was dissolved in ethanol (7 mL), and DeGussa Pd/C (30 mg) was added. H_2 was bubbled through the stirred reaction mixture for 1.5 h. TLC (2:1 light petroleum ether:ethyl acetate) revealed complete disappearance of starting material. Pd/C was removed by filtration over Celite, and the filtrate was concentrated to yield 3-aminopropyl 2,3,4,6-tetra-*O*-acetyl-α-D-mannopyranoside (**9b**). The viscous oil was resuspended in THF (8 mL), and Et_3N (111 μL, 4 equiv) was added. The solution was stirred at 25 °C, and benzoyl chloride (56 mg, 2 equiv) was added slowly. The solution was stirred for 16 h at 25 °C; TLC (1:1 light petroleum ether:ethyl acetate) showed complete conversion to a product which was both UV-active and stained by Hannesian dip. The solution was concentrated and resuspended in CH_2Cl_2 (25 mL). The organic phase was washed with 1.0 M HCl (1 × 20 mL), saturated $NaHCO_3$ (1 × 20 mL), and saturated NaCl (1 × 20 mL), dried ($MgSO_4$), and concentrated. The residue was purified by flash chromatography (2:1 light petroleum ether:ethyl acetate) to yield an amber-colored oil (55 mg, 55%): ^{1}H NMR (600 MHz, $CDCl_3$) δ 1.94−1.98 (m, 2 H), 1.98 (s, 3H), 2.02 (s, 3H), 2.05 (s, 3 H), 2.14 (s, 3H), 3.57−3.60 (m, 3H), 3.78−3.84 (m, 1H), 3.97−4.03 (m, 1H), 4.05−4.09 (dd, 1H, J = 2.6, 12.2 Hz), 4.23−4.29 (dd, 1H, J = 5.4, 12.2 Hz), 4.81 (d, 1H, J = 1.4 Hz), 5.22−5.29 (m, 3H), 6.56 (br s, 1H, N*H*), 7.38−7.48 (m, 3H), 7.76−7.79 (m, 2H) ppm; ^{13}C NMR (75.48 MHz, $CDCl_3$) δ 20.54, 20.65, 20.84, 29.16, 37.59, 62.55, 66.09, 66.49, 68.45, 69.03, 69.38, 97.65, 126.83, 128.54, 131.40, 134.27, 167.55, 169.67, 169.87, 170.04, 170.67 ppm; IR (neat) ν 3395, 2936, 2255, 1748, 1650, 1537, 1370, 1227, 1083, 1049, 912, 731 cm^{-1}; HR FAB MS (pos) calcd for $C_{24}H_{31}NO_{11}$ (MH^+) 510.1975, obsd 510.1982.

3-(Benzylamido)propyl α-D-Mannopyranoside (11). 3-(Benzylamido)propyl 2,3,4,6-tetra-*O*-acetyl-α-D-mannopyranoside (50 mg, 0.098 mmol) was dissolved in 0.1 M NaOMe (4 mL) and stirred at 25 °C for 3 h. The solution was neutralized with Dowex H^+ and concentrated to yield **11** as an amber film (30 mg, 89%): ^{1}H NMR (600 MHz, D_2O) δ 1.94 (m, 2H), 3.46 (t, 2H, J = 5.6 Hz), 3.51−3.64 (m, 3H), 3.69−3.72 (dd, 1H, J = 4.5, 12.1 Hz), 3.76−3.78 (dd, 1H, J = 3.1, 8.6 Hz) 3.81−3.85 (m, 3H), 3.90 (d, 1H, J = 1.6 Hz), 4.84 (s, 1H), 7.48−7.52 (m, 2H), 7.61−7.62 (m, 1H), 7.71−7.74 (m, 2H) ppm; ^{13}C NMR (150 MHz, D_2O) δ 31.30, 40.28, 64.06, 68.63, 69.98, 73.23, 73.81, 75.86, 102.96, 129.99, 131.88, 135.07, 137.08, 173.78, ppm; FAB MS (pos) calcd for $C_{16}H_{23}NO_7$ 341.1, found 342.1 (MH^+), 364.1 (MNa^+).

5-Azidomethyl-*N,N*′-bis[3-*O*-(2,3,4,6-tetra-*O*-acetyl-α-D-mannopyranosyl)propyl]benzene-1,3-dicarboxamide (12). 3-Azidopropyl 2,3,4,6-tetra-*O*-acetyl-α-D-mannopyranoside (250 mg, 0.58 mmol) was dissolved in ethanol (5 mL), and DeGussa Pd/C (70 mg) was added. H_2 was bubbled through the reaction solution for 3 h at 25 °C. The Pd/C was removed by filtration over Celite and the filtrate concentrated to yield 3-aminopropyl 2,3,4,6-tetra-*O*-acetyl-α-D-mannopyranoside (**9b**). The crude material was resuspended in THF (12 mL), and Et_3N (324 μL, 4 equiv) was added. 5-Azidomethyl-1,3-dicarbonylbenzene dichloride (58 mg, 0.26 mmol, 0.45 equiv) was added and the resulting solution stirred for 16 h at 25 °C. The reaction mixture was concentrated and resuspended in CH_2Cl_2. The organic phase was washed with 1.0 M HCl (1 × 20 mL), saturated $NaHCO_3$ (1 × 20 mL), and brine (1 × 20 mL), dried ($MgSO_4$), and concentrated. The crude material was purified via flash chromatography (2:1 light petroleum ether:ethyl acetate) to yield **12** as an amber oil (120 mg, 53%): ^{1}H NMR (600 MHz, $CDCl_3$) δ 1.86−1.97 (m, 2H), 1.95 (s, 6H), 2.00 (s, 6H), 2.03 (s, 6H), 2.11 (s, 6H), 3.48−3.58 (m, 4H), 3.75−3.79 (m, 2H), 3.96−3.98 (m, 2H), 4.05−4.08 (m, 2H), 4.21−4.24 (dd, 2H, J = 5.4, 12.2 Hz), 4.43 (s, 2H), 4.78 (d, 2H, J = 1 Hz), 5.18−5.24 (m, 6H), 6.98 (t, 2H, J = 5.8 Hz), 7.88 (s, 2H), 8.17 (s, 1H) ppm; ^{13}C NMR (150.86 MHz, $CDCl_3$) δ 20.69, 20.74, 20.88, 29.33, 37.60, 54.04, 60.41, 62.71,

66.28, 68.57, 69.21, 69.53, 97.77, 125.11, 129.57, 135.47, 137.03, 166.51, 169.79, 170.12, 170.20, 170.88 ppm; IR (film) ν 3413, 3058, 2959, 2101, 1745, 1651, 1538, 1434, 1370, 1260, 1136, 1084, 1049, 739 cm^{-1}; HR FAB MS (pos) calcd for $C_{43}H_{57}N_5O_{22}$ (MH^+) 996.3573, obsd 996.3583.

5-Azidomethyl-*N,N′*-bis[3-(*O*-α-D-mannopyranosyl)propyl]benzene-1,3-dicarboxamide (13). 5-Azidomethyl-*N,N′*-bis[3-*O*-(2,3,4,6-tetra-*O*-acetyl-α-D-mannopyranosyl)propyl]benzene-1,3-dicarboxamide (120 mg, 0.12 mmol) was dissolved in 0.1 M NaOMe (10 mL) and stirred at 25 °C for 2 h. The solution was neutralized with Dowex H^+ resin and concentrated. The crude material was purified by flash chromatography (1:1:0.1 ethyl acetate:ethanol:H_2O) to yield **13** as a white foam (63 mg, 79%): ^{1}H NMR (600 MHz, D_2O) δ 1.93−1.95 (m, 4 H), 3.48−3.52 (t, 4H, J = 6.5 Hz), 3.58−3.62 (m, 6H), 3.69−3.72 (dd, 2H, J = 4.3, 11.9 Hz), 3.75−3.77 (dd, 2H, J = 3.3, 9.0 Hz), 3.80−3.84 (m, 3H), 3.90−3.91 (dd, 2H, J = 1.8, 3.2 Hz), 4.55 (s, 2 H), 4.83 (s, 2 H), 7.88 (s, 2H), 8.03 (s, 1H) ppm; ^{13}C NMR (150 MHz, D_2O) δ 31.26, 40.42, 56.60, 64.08, 68.57, 69.98, 73.26, 73.83, 75.89, 102.97, 128.41, 132.78, 138.22, 140.44, 172.26 ppm; FAB MS (pos) calcd for $C_{27}H_{41}N_5O_{14}$ 659.3, found 660.2 (MH^+), 682.2 (MNa^+).

***N,N′,N″*-Tris[3-*O*-(2,3,4,6-tetra-*O*-acetyl-α-D-mannopyranosyl)-propyl]benzene-1,3,5-tricarboxamide (14).** 3-Azidopropyl 2,3,4,6-tetra-*O*-acetyl-α-D-mannopyranoside (220 mg, 0.51 mmol) was dissolved in ethanol (5 mL). DeGussa Pd/C was added, and H_2 was bubbled through the reaction mixture. Pd/C was removed by filtration over Celite, and the filtrate was concentrated. Crude **9b** was redissolved in THF, and Et_3N (554 μL, 8 equiv) was added. After 20 min 1,3,5-benzenetricarbonyl trichloride (45 mg, 0.31 equiv) was added, and the reaction mixture was stirred for 16 h at 25 °C. The solution was concentrated, resuspended in CH_2Cl_2, washed with 1.0 M HCl (1 × 20 mL), saturated $NaHCO_3$ (1 × 20 mL), and brine (1 × 20 mL), dried ($MgSO_4$), and concentrated. Crude material was purified via flash chromatography (2:1:0.2 light petroleum ether:ethyl acetate:methanol) to yield trivalent mannoside **14** as a white foam (75 mg, 32% yield for two steps): ^{1}H NMR (600 MHz, $CDCl_3$) δ 1.97 (m, 6H), 1.98 (s, 9H), 2.01 (s, 9H), 2.06 (s, 9H), 2.15 (s, 9H), 3.52−3.56 (m, 9H), 3.65−3.69 (m, 3H), 3.79−3.84 (m, 3H), 4.06−4.08 (m, 3H), 4.12−4.15 (m, 3H), 4.25−4.29 (dd, 3H, J = 5.4, 12.2 Hz), 4.81 (s, 3H), 5.23−5.28 (m, 9H), 6.97 (br s, 3H), 8.38 (s, 3H) ppm; ^{13}C NMR (75.48 MHz, $CDCl_3$) δ 20.54, 20.66, 20.74, 20.80, 20.88, 29.32, 37.31, 62.49, 62.64, 65.97, 66.08, 66.19, 68.29, 68.33, 68.72, 69.06, 69.49, 70.00, 97.70, 128.27, 135.03, 165.95, 169.06, 169.74, 169.92, 169.94, 170.14, 170.74, 170.96 ppm; IR (neat) ν 3413 (br), 1739, 1658, 1537, 1434, 1370, 1226, 1083, 1049, 738 cm^{-1}; HR FAB$^+$ MS calcd for $C_{60}H_{81}N_3O_{33}$ (MH^+) 1372.4831, obsd 1372.4768.

***N,N′,N″*-Tris[3-*O*-(α-D-mannopyranosyl)propyl]benzene-1,3,5-tricarboxamide (15).** *N,N′,N″*-Tris[3-*O*-(2,3,4,6-tetra-*O*-acetyl-α-D-mannopyranosyl)propyl]benzene-1,3,5-tricarboxamide (80 mg, 0.06 mmol) was dissolved in 0.1 M NaOMe (3 mL). The solution was stirred at 25 °C for 24 h and then neutralized with Dowex H^+ resin. The resin was removed by gravity filtration, and the solution was concentrated. The crude material was purified by size-exclusion chromatography (Sephadex G-10 resin) to yield **15** as a white foam (32 mg, 64%): ^{1}H NMR (600 MHz, D_2O) δ 1.96−1.98 (m, 6H), 3.51−3.54 (t, 6H, J = 6.7 Hz), 3.59−3.64 (m, 9H), 3.70−3.73 (dd, 3H, J = 4.2, 12.1 Hz), 3.75−3.77 (dd, 3H, J = 2.6, 8.1 Hz), 3.81−3.86 (m, 9H), 3.91 (s, 3H), 4.85 (s, 3H), 8.24 (s, 3H) ppm; ^{13}C NMR (150 MHz, D_2O) δ 31.27, 40.51, 64.11, 68.60, 70.00, 73.27, 73.84, 75.92, 102.98, 131.59, 138.31, 171.79 ppm; FAB MS (pos) calcd for $C_{36}H_{57}N_3O_{21}$ 867.3, found 890.3 (MNa^+), 726.3, 562.3.

5-Azidomethyl-*N,N′*-bis[*N,N′*-bis[3-*O*-(2,3,4,6-tetra-*O*-acetyl-α-D-mannopyranosyl)propyl]-1-phenylmethyl-3,5-dicarboxamide]benzene-1,3-dicarboxamide (16). Peracetylated bivalent dendron **12** (200 mg, 0.2 mmol) was dissolved in ethanol (10 mL), and Pd/C (35 mg) was added. H_2 was bubbled through the reaction mixture. Upon complete disappearance of starting material, catalyst was removed by vacuum filtration over Celite, and the filtrate was concentrated. Reduced dendron **12b** was resuspended in THF, and Et_3N (112 μL, 4 equiv) was added. After 10 min, 5-azidomethyl-1,3-dicarbonylbenzene dichloride (25 mg, 0.45 equiv) was added. The reaction mixture was stirred at 25 °C for 16 h. Solvent was removed in vacuo, and the residue was resuspended in CH_2Cl_2. The organic phase was washed with 1.0 M HCl (1 × 20 mL), saturated $NaHCO_3$ (1 × 20 mL), and brine (1 × 20 mL), dried ($MgSO_4$), and concentrated. The crude material was purified by silica chromatography (1:1:0.5 light petroleum ether:ethyl acetate:methanol) to yield **16** as a pale yellow foam (85 mg, 40%): ^{1}H NMR (500 MHz, $CDCl_3$) δ 1.93 (m, 8H), 1.97 (s, 12 H), 2.03 (s, 12H), 2.06 (s, 12H), 2.13 (s, 12H), 3.51−3.54 (m, 12H), 3.80 (m, 4H), 3.99 (m, 4H), 4.08−4.12 (m, 4H), 4.23−4.26 (m, 4H), 4.41−4.43 (m, 4H), 4.47 (s, 2H), 4.80 (s, 4H), 5.20−5.26 (m, 12H), 6.97 (br s, 2H), 7.37 (br s, 4H), 7.74−7.87 (m, 9H) ppm; ^{13}C NMR (75.48 MHz, $CDCl_3$) δ 20.67, 20.72, 20.87, 29.12, 29.65, 33.84, 37.31, 49.08, 54.06, 62.46, 65.98, 66.02, 66.13, 68.38, 69.10, 69.45, 97.59, 129.08, 134.60, 137.58, 139.12, 156.94, 167.13, 169.69, 170.08, 170.17, 170.20, 170.80 ppm; IR (neat) ν 3383, 2936, 2254, 2102, 1746, 1650, 1538, 1432, 1370, 1225, 1050, 909, 730, cm^{-1}; FAB MS (pos) calcd for $C_{95}H_{121}N_9O_{46}$ 2124.7, obsd 2125.7 (MH^+).

5-Azidomethyl-*N,N′*-bis[*N,N′*-bis[3-*O*-(α-D-mannopyranosyl)propyl]-1-phenylmethyl-3,5-dicarboxamide]benzene-1,3-dicarboxamide (17). *5*-Azidomethyl-*N,N′*-bis[*N,N′*-bis[3-*O*-(2,3,4,6-tetra-*O*-acetyl-α-D-mannopyranosyl)propyl]-1-phenylmethyl-3,5-dicarboxamide]benzene-1,3-dicarboxamide (50 mg, 0.023 mmol) was dissolved in 0.1 M NaOMe (5 mL) and stirred at 25 °C for 24 h. The reaction was neutralized with Dowex H^+ and concentrated. The crude residue was purified by size-exclusion chromatography (Sephadex G-25 resin) to yield **17** as clear oil (24 mg, 63%): ^{1}H NMR (600 MHz, D_2O) δ1.76−1.78 (m, 4H), 1.87−1.89 (m, 4H), 3.30−3.33 (m, 8H), 3.39−3.82 (m, 32 H), 4.34−4.57 (m, 6H), 4.77−4.78 (m, 4H), 7.70 (s, 2H), 7.73 (s, 2H), 7.77 (s, 2H), 7.82 (s, 1H), 7.87 (s, 1H), 7.89 (s, 1H) ppm; ^{13}C NMR (150 MHz, D_2O) δ 26.35, 31.28, 40.35, 46.17, 64.06, 68.47, 69.98, 73.27, 73.87, 75.88, 102.97, 127.66, 132.03, 133.09, 137.86, 172.02 ppm; MALDI-TOF MS calcd for $C_{63}H_{89}N_9O_{30}$ 1451.6, obsd 1474.5 (MNa^+).

***N,N′,N″*-Tris[*N,N′*-bis[3-*O*-(2,3,4,6-tetra-*O*-acetyl-α-D-mannopyranosyl)propyl]-1-phenylmethyl-3,5-dicarboxamide]benzene-1,3,5-tricarboxamide (18).** Peracetylated bivalent dendron **12** (190 mg, 0.19 mmol) was dissolved in ethanol (6 mL), and DeGussa Pd/C (45 mg) was added. H_2 was bubbled through the reaction mixture during 2 h. Pd/C was removed by filtration over Celite, and the filtrate was concentrated. The residual oil **12b** (150 mg) was dissolved in THF, and Et_3N (216 μL, 10 equiv) was added. 1,3,5-Benzenetricarbonyl trichloride (13 mg, 0.065 mmol, 0.33 equiv) was added and the reaction mixture refluxed for 18 h. The solution was concentrated and redissolved in CH_2Cl_2, washed with 1.0 M HCl (1 × 20 mL), saturated $NaHCO_3$ (1 × 20 mL), and brine (1 × 20 mL), dried ($MgSO_4$), and concentrated. The crude product was purified by silica chromatography (4:1:0.5 ethyl acetate:ethanol:H_2O) to yield **18** as a gold oil (85 mg, 54%): ^{1}H NMR (400 MHz, $CDCl_3$) δ 1.98−2.16 (m, 84H), 3.55−3.61 (m, 18H), 3.82 (m, 6H) 3.97−4.08 (m, 6H), 4.11−4.13 (m, 6H), 4.24−4.28 (m, 6H), 4.82−4.83 (m, 6H), 5.23−5.30 (m, 18H), 7.83−8.52 (m, 12H) ppm; ^{13}C NMR (75.48 MHz, $CDCl_3$) δ 20.69, 20.87, 29.09, 29.17, 29.23, 29.65, 37.36, 37.41, 37.68, 62.45, 62.51, 62.55, 62.58, 62.62, 62.68, 66.03, 66.03, 66.09, 66.21, 66.24, 68.34, 68.36, 68.75, 69.02, 69.06, 69.16, 69.20, 69.43, 70.00, 97.66, 97.68, 127.13, 128.34, 131.06, 132.47, 134.23, 135.81, 136.19, 169.74, 169.98, 170.13, 170.15, 170.77, 170.79, 170.91 ppm; FAB MS (pos) calcd for $C_{138}N_9O_{69}H_{177}$ 3064.2, obsd 3066.4 (MH^+).

***N,N′,N″*-Tris[*N,N′*-bis[3-*O*-(α-D-mannopyranosyl)propyl]-1-phenylmethyl-3,5-dicarboxamide]benzene-1,3,5-tricarboxamide (19).** Peracetylated hexavalent mannoside **18** (52 mg, 0.017 mmol) was dissolved in 0.1 M NaOMe (15 mL) and stirred at 25 °C for 36 h. The solution was neutralized with Dowex H^+ and concentrated. The crude product was applied to a G-50 Sephadex column and eluted with H_2O to yield **19** as a white foam (26 mg, 75%): ^{1}H NMR (600 MHz, D_2O) δ 1.81−1.82 (m, 6H), 1.92−1.94 (m, 6H), 3.34−3.92 (m, 60H), 4.50−4.52 (m, 6H), 4.77 (m, 3H), 4.84 (m, 3H), 7.74 (s, 3H), 7.74−7.83 (m, 6H), 8.27−8.37 (m, 3H) ppm; ^{13}C NMR (150 MHz, D_2O) δ 26.40, 31.30, 34.10, 40.41, 46.27, 62.49, 64.08, 68.49, 69.98, 73.27, 73.84, 75.88, 102.95, 127.77, 131.99, 137.61, 142.40, 171.52 ppm; MALDI-TOF MS calcd for $C_{90}H_{129}N_9O_{45}$ 2057.8, obsd 2080.1 (MNa^+).

Calorimetry. Titration microcalorimetry was performed using the MicroCal Omega titration microcalorimeter. Details of instrument

design and data analysis are described elsewhere.[74] Briefly, a solution of concanavalin A (0.28−0.78 mM) in a buffer of 50 mM dimethyl glutarate, 250 mM NaCl, 1 mM $CaCl_2$, and 1 mM $MnCl_2$ at pH 5.2 was placed in the sample cell. Glycodendrimer solutions ([mannose] = 11.3−24.9 mM) in a buffer identical to that used for protein solutions were added in 25−40, 2.0−2.2-μL increments during 30 s, with 3-min intervals between injections. Each calorimetric titration was performed at a sample cell temperature between 26 and 30 °C. Protein concentrations were determined spectrophotometrically using an extinction coefficient of $\epsilon_{280} = 1.24$ for a 1 mg/mL solution. Carbohydrate concentrations were determined using the phenol−sulfuric acid charts of DuBois.[75]

The heat evolved upon each injection was digitally recorded, and the data were integrated to generate a titration curve upon completion of the experiment. The stoichiometry of the association, *n*, binding constant, K_c, and the change in enthalpy, ΔH, were obtained from a nonlinear least-squares fit using the Origin software program. All data are presented on a valency-corrected basis.

(74) Wiseman, T.; Williston, S.; Brandts, J. F.; Lin, L.-N. *Anal. Biochem.* **1989**, *179*, 131.

(75) Dubois, M.; Gilles, K. A.; Hamilton, J. K.; Rebers, P. A.; Smith, F. *Anal. Chem.* **1956**, *28*, 350.

Hemeagglutination. Nonspecific binding to microtiter plates was blocked by addition of a solution of BSA in PBS and BSA (50 μL). Carbohydrate solution of a known concentration (50 μL) was added to the first well and serially diluted. Concanavalin A solution (50 μL) was added to all wells, and the plate was incubated at 37 C for 2 h. A 2% solution of EDTA-anticoagulated porcine red blood cells (50 μL) was added to each well. Plates were read following a 1 h incubation.

Acknowledgment. We are grateful to Dr. G. Dubay for the mass spectroscopy. S.M.D. acknowledges the NIH Biological Chemistry Training Program for funding. E.J.T. acknowledges the support of the NIH (GM 48653) J.H.N. acknowledges the U.K. BBSRC (49/B08307) for support. J.H.N. thanks Prof. J. R. Helliwell and Prof. S. W. Homans for encouragement and helpful discussions.

Supporting Information Available: Copies of ^{1}H and ^{13}C NMR spectra for compounds **11**, **13**, **15**, **17**, and **19** (PDF). This material is available free of charge via the Internet at http://pubs.acs.org.

JA991729E